

An In-Depth Study of Magnesium Composite in Various Corrosive Media: Insight in Orthopedic Implant



Adedotun Adetunla*, Bernard Adaramola, Omolayo Ikumapayi, Ebenezer O. Ige, Sunday Afolalu

Department of Mechanical & Mechatronics Engineering, Afe Babalola University, Ado Ekiti 23401, Nigeria

Corresponding Author Email: adedotunla.adedotun@abuad.edu.ng

<https://doi.org/10.18280/rcma.320602>

ABSTRACT

Received: 30 August 2022

Accepted: 29 November 2022

Keywords:

calcium carbonate, corrosion rate, impact test, metal matrix composite, orthopedic implant

The majority of the properties required for orthopedic implant operation are demonstrated by magnesium and its alloys, however, the metal degrades rapidly in the body's environment. Therefore, a magnesium-based metal matrix composite capable of safely and gradually degrading in the body within the required healing time is required, thereby eliminating the need for a second surgery. The degradability of this newly formed alloy was done via corrosion test of this alloy in various corrosive media namely, H₂O, NaCl, Urine, Blood, and Plasma. Three samples A (50% reinforcement), B (25% reinforcement), and C (No reinforcement) of grade AZ31B Magnesium alloy and Calcium Carbonate powder reinforcement were developed via stir-casting technique. The impact strength of this alloy was carried out by using Charpy Impact Tester, while the microstructural characterization was determined by Scanning Electron Microscope (SEM).

1. INTRODUCTION

Magnesium is a prevalent element in the earth's crust, although it accounts for a small percentage of the total. It is found all over the world, even though it is present only in its combined forms. Magnesite (MgCO₃), Dolomite (MgCO₃CaCO₃), Carnallite (KClMgCl₂·6H₂O), and seawater are the most common compounds [1]. Magnesium is the lightest metal, weighing between 1.74 and 2.0 grams per cubic centimeter which is 33 percent lighter than aluminum and 77 percent lighter than steel. According to Yusop et al. [2] the physical and mechanical properties of magnesium (i.e., elastic modulus of 41–45 GPa) is closely comparable with those of cortical and cancellous bones which would decrease the occurrence of stress shielding. A combination of its mechanical, biodegradable, and biocompatible properties makes it a suitable choice for load bearing applications in the body. However, it is worth noting that the degradation rate of pure magnesium is extremely high in physiological environment restraining their applications for implant applications which is exposed to body fluid [3, 4].

Metallic materials have been the major constituent of orthopedic implants as a result of their mechanical strength. This has led researchers to develop metallic materials with high strength and low density, which is capable of safely degrading in the body, hence eliminating the need for second surgery. A major material of interest is the Magnesium (Mg) and its alloy, as studies have revealed that Mg can safely degrade in the body of human [5], thus making it highly considered as a material for orthopedic implant. Human bones are found similar to Mg alloys in terms of modulus and density [6], however, Mg alloys are difficult to process and they easily corrode. However, they corrode easily and very difficult to

process [7, 8]. Figure 1 presents some existing clinical applications of Mg alloys.

Mechanical properties such as tensile and hardness of Mg alloy has limited its use in the medical field, such as Mg alloy screws being only used for unload-bearing positions in clinic. Another major use of Mg alloy is its usage as a bone screw that helps to fasten the bones together, therefore, great importance should be given to Mg alloys since they are crucial in cardiovascular surgeries and fixation of fractures. Mg has good creep resistance, high ductility.

To alter the properties of pure magnesium, alloying materials are employed. Magnesium is a chemically active element that, when mixed with other metal alloying elements, can produce intermetallic compounds. Composite materials are ones that are made up of two or more fundamentally different components that work together to create qualities that are superior to those provided by either component alone [9]. They are materials that are made up of two or more different types of materials that do not react with each other, intended to increase mechanical qualities or to create materials that have both functional and structural properties. Various works have attempted to reinforce Magnesium with other element in order to improve its mechanical properties.



(a)

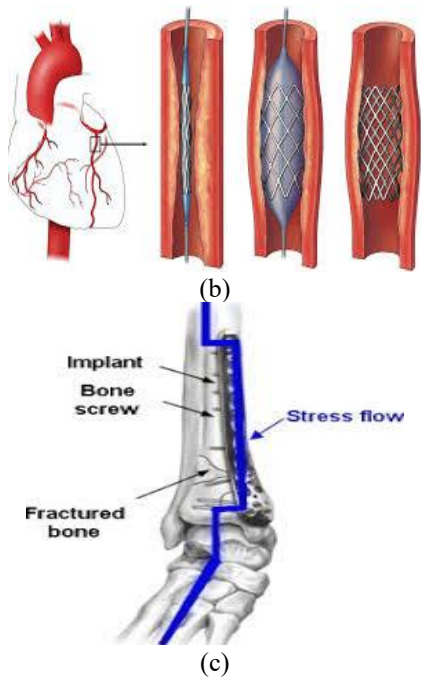


Figure 1. Existing clinical applications of magnesium alloy: (a) MAGNEZIX screw, (b) Coronary stent, (c) Orthopedic implants [10]

Zhang et al. [11] used a novel surface modification method to improve the corrosion resistance, blood compatibility and cytocompatibility of the magnesium alloy. The alloy was treated by NaOH and then 16-Phosphonohexadecanoic acid was added to the modified surface by self-assembly. Polyethylene glycol, fibronectin and fibronectin/heparin were also immobilized on the alloy, results obtained showed improved corrosion resistance, blood compatibility and cytocompatibility to endothelial cells.

Adetunla and Akinlabi [12] created four AZ31 magnesium composites reinforced with Fly ash, Palm kernel shell ash, Ti-6Al-4V, and 304 stainless steel powders using the friction stir processing method with a view to improve corrosion resistance, wear performance and other mechanical properties. The manufactured 304 stainless steel samples were the most ideal because they had the best corrosion resistance among the corrosive media utilized. Rajkumar et al. [13] studied the effects of bio and tribo modification of magnesium-calcium carbonate biomaterials using Tungsten Sulphide and Hexagonal Boron Nitride respectively, they observed weight loss as the composites were immersed in a simulated body fluid (SBF) at 37°C. However, the rate of mass loss degradation could not be decreased by the addition of these modifiers. The study aims to develop a Magnesium based metal matrix composite capable of safely and gradually degrading in various corrosive media typically found in human body, which attempts to eliminate the need for a secondary surgery. The results obtained from this study are discussed extensively.

2. METHODOLOGY

The base metal employed in the research is the AZ31 Magnesium (Mg) alloy with Calcium Carbonate powder (CaCO_3) used as its reinforcement. The Mg alloy was procured as a square plate weighing 450g with length and breadth 100mm each, and 3mm thickness, while 500g of the Calcium

Carbonate Powder (CaCO_3) was acquired. The composition of the CaCO_3 powder in the casting process were varied according to weight, resulting in three cast samples A, B and C as seen in Figure 2. Table 1 shows the varied compositions of the cast AZ31Mg/ CaCO_3 composites.

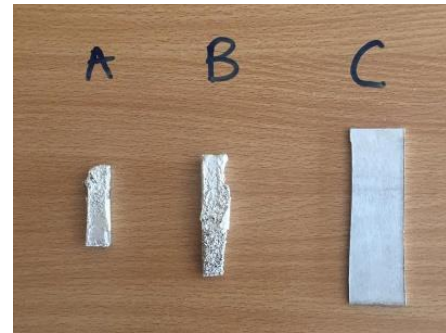


Figure 2 Stir-cast AZ31BMg- CaCO_3 samples

Table 1. Varied composition of the fabricated Az31Mg/ CaCO_3 composite

Sample	AZ31BMg		CaCO ₃	
	(%)	(g)	(%)	(g)
A	50	16.35	50	16.35
B	75	17.95	25	13.46g
C	100	15.7	-	-

To determine the performance of the magnesium metal matrix composite under shock loading, the samples were prepared according to the following dimensions. Sample A (50% reinforced), Sample B (25% reinforced) and Sample C (0% reinforced) were machined to various dimensions. V-Notches of depth 2mm were engrooved into the samples using a triangular file. The test was performed using a Charpy Impact Tester shown in Figure 3 at room temperature observing all necessary precautions. The hammer is suspended at a 45-degree angle to the horizontal plane. The specimen is hammered directly on the opposite side of the notch when the arm is released, causing the specimen to fracture. Weight reduction method was adopted to determine the corrosion resistance of the composite samples in H_2O (p), NaCl (s), Urine (u), Blood (o), and Plasma (m). Specimens were cut from samples A (50% reinforcement), B (25% reinforcement), and C (0% reinforcement) respectively. Fifteen samples overall were obtained after the preparation process, five each of the compositions A, B, and C. Approximately 50ml of each medium was poured into fifteen plastic containers appropriately labeled with the sample composition letter and medium symbol as subscripts as seen in Table 2. The masses of the samples were measured for weight loss over a period of 48 days with intervals of 5 days each. Figure 4 shows the samples in their respective corrosive media.

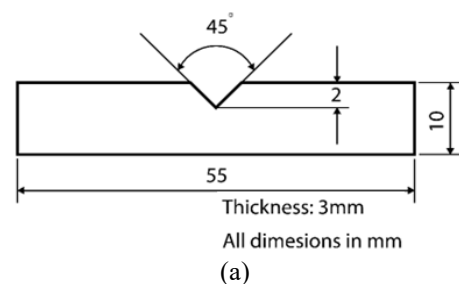




Figure 3. (a) Schematic diagram of sample for impact test, (b) Samples before fracture



Figure 4. Corrosive media containing AZ31Mg-CaCO₃ samples: Plasma, Blood, Urine, NaCl and H₂O

Table 2. Preparation of corrosion test

Medium	Sample	Mass of container (g)	Volume of medium (ml)	Mass of container + medium (g)	Mass of container + medium + sample (g)
H ₂ O	Ap	9.77	50	71.98	72.6
	Bp	9.73	50	84.81	86.05
	Cp	9.72	50	81.17	81.75
NaCl	As	9.73	50	91.44	91.98
	Bs	9.59	50	96.19	97.49
	Cs	9.71	50	96.94	97.42
URINE	Au	9.72	50	80.88	81.53
	Bu	9.64	50	80.49	81.95
	Cu	9.65	50	71.31	71.93
BLOOD	Ao	9.72	50	80.13	80.73
	Bo	9.74	50	78.6	79.78
	Co	9.5	50	87.73	88.37
PLASMA	Am	9.76	50	71.83	72.46
	Bm	9.88	50	73.26	74.07
	Cm	9.65	50	69.96	70.51

3. RESULTS AND DISCUSSION

3.1 Scanning Electron Microscope (SEM)

The surface of the parent material, AZ31 Magnesium alloy, was analysed using the Phenom ProX SEM machine with magnifications of 100 μ m, and 50 μ m as shown in Figure 5. The darker precipitates in the as-received alloy have a fine continuous distribution across the grains and inside grain borders, with grain boundaries that are elongated or stretched, indicating that the cell configuration of the precipitates is eutectic. The outlined white spot in Figure 4 indicates the presence of undissolved elements or impurities in the alloy. However, it is negligible as its occurrence is rare throughout the microstructure.

Figure 6 shows the microstructural imaging of Sample A (50% reinforced).

The outlined white spot in Figure 6b indicates the presence of the undissolved CaCO₃ reinforcement in the matrix due to differences in their melting point. As seen in the parent material, its appearance is also negligible, therefore a fine distribution of the reinforcement throughout the matrix was obtained. The microstructural imaging of Sample B (25% reinforced) is represented in Figure 7. There is an occurrence of microstructural defect like tunnel holes as observed in Sample A. However, less undissolved particles and a finer distribution than the 50% reinforced sample can be observed from the image. Due to the dynamic recrystallization which occurs at the stir zone, it has been established that grain refinement during the process can lead to enhanced

mechanical properties, such as the hardness value, using the Hall-Petch equation [14].

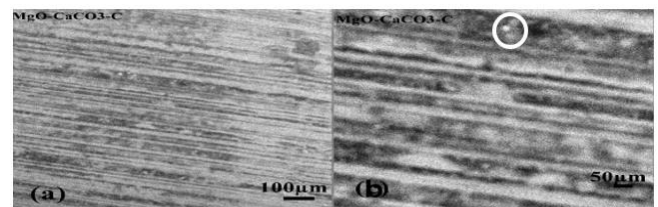


Figure 5. SEM micrograph of sample C (control sample)

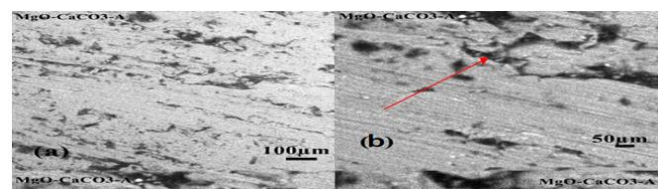


Figure 6. SEM micrograph of sample A (50% reinforced)

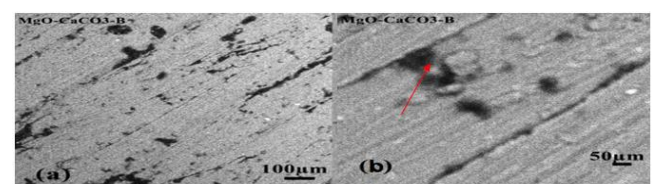


Figure 7. SEM micrograph of sample B (25% reinforced)

3.2 Impact test result

After sample preparations, the samples were fractured by the Charpy Impact Tester. Figure 8 shows the samples after fracture. The types of fracture witnessed in samples A and B are indicators of ductility of the material.



Figure 8. Impact samples after fracture

Table 3 displays the results of the impact test carried out on samples A, B, and C via the Charpy Impact Tester. The tested specimen absorbs the energy of the swinging hammer therefore declining its velocity. Impact strength is mathematically represented in Eq. (1). Sample B was observed to have the highest impact strength compared to the other specimens which is in agreement with similar studies [15-17].

$$\text{Impact Strength} = \frac{E}{A} \quad (1)$$

where:

E= Energy required to fracture the specimen in Joules.

A= Surface Area of the specimen in m².

3.3 Corrosion behavior

The masses of the fabricated samples were measured for weight loss over a period of 48 days with intervals of 5 days each. Data from Table 4 shows that sample B immersed in H₂O experienced the greatest weight loss as compared to other samples. Sample A which was the best performing sample in H₂O with the least corrosion rate of 0.02458g/days started out as the fastest corroding specimen in H₂O as seen on the table.

However, it was surpassed by Sample B with a corrosion rate of 0.06396g/days and Sample C corroded at a rate of 0.02833g/days. The samples immersed in NaCl experienced relatively low amounts of weight loss as seen in Figure 9. The slowest corrosion rate was observed from Sample B immersed in NaCl with a value of 0.01708g/days. Furthermore, Samples A and C surpassed Sample B with corrosion rates of 0.02g/days and 0.01979g/days respectively. Samples A, B and C corroded at rates (0.2208g/days, 0.01729g/days, and 0.04042g/days) respectively according to the figure. Sample C experienced a significant weight loss in urine as seen in Figure 10, possibly due to undetermined reactions between the material and the medium which led to this rapid corrosion.

Like H₂O, significant weight losses were observed in blood. Samples A, B, and C experienced corrosion rates of 0.03g/days, 0.02576g/days, and 0.02273g/days respectively. As observed from Table 5, all three samples corroded at almost equal rates during the first two weeks of testing and then a sudden increase in corrosion rates was experienced from samples A and B. Furthermore, low corrosion rates (0.01788g/days, 0.03121g/days, and 0.01727g/days) of Samples A, B, and C respectively were experienced in plasma, Figure 10 shows that Sample B actively degraded in the medium compared to the other samples. Observations made from the Table 4 and Figure 11 shows that Sample A was averagely the slowest degrading sample across all corrosive media. Consequently, Sample B was averagely the worst performing sample amongst all three samples. Specifically, according to immersion in water which is largely found in human, the greatest corrosion was observed in Sample B immersed in H₂O with a corrosion rate of 0.06395g/days while the least corrosion was observed in Sample A immersed in NaCl solution with a rate of 0.01708g/days (0.0001752g/year) as shown in Table 6. Therefore, the reinforcements improved the corrosion resistance of the AZ31B Mg alloy.

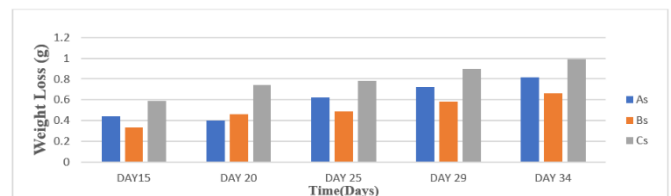


Figure 9. Corrosion behavior in NaCl

Table 3. Impact test result

S/N	Sample	Energy absorbed (Joules)	Surface area of specimen (mm ²)	Impact strength (J/mm ²)
1	A	135	1490	0.0906
2	B	186	1490	0.1248
3	C	136	1490	0.0913
Average impact strength			0.1022 J/mm ²	

Table 4. Corrosion behavior of samples immersed in H₂O

Sample	Day 6	Day 11	Day 15	Day 20	Day 25	Day 29	Day 34	Day 39	Day 43	Day 48
Ap	0.47	0.6	0.74	0.91	0.99	1.14	1.24	1.34	1.54	1.65
Bp	0.4	0.54	0.68	0.87	0.98	1.14	1.24	1.31	2.09	3.47
Cp	0.34	0.48	0.64	0.84	0.92	1.07	1.17	1.26	1.44	1.7

Table 5. Corrosion behavior of samples immersed in blood

Sample	Day 6	Day 11	Day 15	Day 20	Day 25	Day 29	Day 34	Day 38	Day 43	Day 48
Ao	-	-	0.2	0.46	0.57	0.7	0.84	0.95	1.05	1.19
Bo	-	-	0.2	0.46	0.58	0.72	0.86	0.96	1.04	1.05

Co	-	-	0.19	0.34	0.36	0.45	0.57	0.69	0.81	0.94
----	---	---	------	------	------	------	------	------	------	------

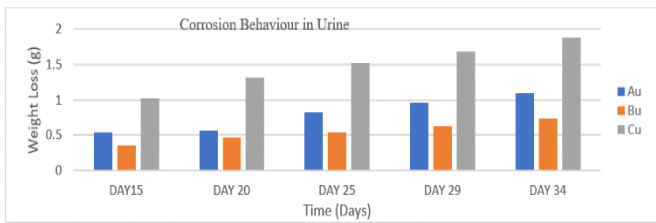


Figure 10. Corrosion behavior in urine

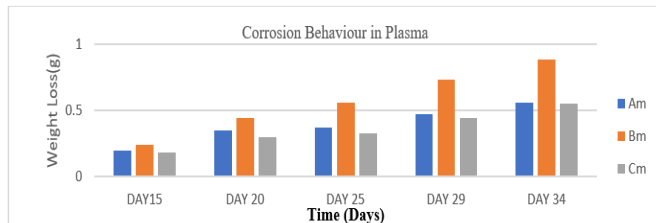


Figure 11. Corrosion behavior in plasma

Table 6. Corrosion rate of specimen in various media

	H ₂ O	NaCl	Blood	Plasma
Sample A	0.02458	0.02	0.03	0.01788
Sample B	0.06390	0.01708	0.02576	0.03131
Sample C	0.02833	0.01979	0.02273	0.01727

4. CONCLUSIONS

The AZ31B Mg alloy was successfully strengthened with CaCO₃ powder via stir casting technique in this study. The SEM analysis, Impact test were carried out on this newly formed alloy which shows sample B with the highest impact strength of 0.1248 J/mm² closely followed by Sample A. Lastly, the corrosion rate of this alloy was investigated in various corrosive media. The corrosion resistance of the reinforced samples was improved with sample A (50% base metal/ 50% reinforcement) displaying the slowest degradation at a rate of 0.01708g/days in NaCl, 0.06396g/days in H₂O, 0.02576g/days in blood and 0.03121g/days in plasma.

This shows that the composition of sample A is an appropriate metal matrix mixture when considering Magnesium composite for orthopedic implants. According to the findings, stir-cast AZ31B Mg/CaCO₃ has a good chance of being employed in orthopedic applications where corrosion resistance is critical.

ACKNOWLEDGMENT

The authors wish to acknowledge the Strength of Material Laboratory in Afe Babalola University, Ado, Nigeria, where the tests were carried out.

REFERENCES

[1] Barmouz, M., Asadi, P., Besharati Givi, M.K., Taherishargh, M. (2011). Investigation of mechanical properties of Cu/SiC composite fabricated by FSP: Effect of SiC particles' size and volume fraction. *Mater. Sci.*

Eng. A, 528(3): 1740-1749. <https://doi.org/10.1016/j.msea.2010.11.006>

[2] Yusop, A.H., Bakir, A.A., Shaharom, N.A., Abdul Kadir, M.R., Hermawan, H. (2012). Porous biodegradable metals for hard tissue scaffolds: A review. *Int. J. Biomater.*, 2012: 641430. <https://doi.org/10.1155/2012/641430>

[3] Jones, J.C., Topoleski, L.D.T., Tsao, A.K. (2017). *Biomaterials in orthopaedic implants. Mechanical Testing of Orthopaedic Implants.* Elsevier Ltd., pp. 17-32. <https://doi.org/10.1016/B978-0-08-100286-5.00002-0>

[4] Baneshi, N., Moghadas, B.K., Adetunla, A., et al. (2021). Investigation the mechanical properties of a novel 3D multicomponent scaffold coated with a new bio-nanocomposite for bone tissue engineering: Fabrication, simulation and characterization. *J. Mater. Res. Technol.*, 15: 5526-5539. <https://doi.org/10.1016/j.jmrt.2021.10.107>

[5] Chan, C., Carson, L., Smith, G.C., Morelli, A., Lee, S. (2017). Enhancing the antibacterial performance of orthopaedic implant materials by fibre laser surface engineering. *Appl. Surf. Sci.*, 404: 67-81. <https://doi.org/10.1016/j.apsusc.2017.01.233>

[6] Höhn, S., Virtanen, S., Boccaccini, A.R. (2018). Protein Adsorption on Magnesium and its alloys: A review. *Appl. Surf. Sci.*, 464: 212-219. <https://doi.org/10.1016/j.apsusc.2018.08.173>

[7] Tahreen, N., Zhang, N.F., Pan, F.S., Jiang, X.Q., Li, D.Y., Chen, D.L. (2018). Strengthening mechanisms in magnesium alloys containing ternary I, W and LPSO phases. *J. Mater. Sci. Technol.*, 34(7): 1110-1118. <https://doi.org/10.1016/j.jmst.2017.12.005>

[8] Turan, M.E., Sun, Y., Aydin, F., Zengin, H., Turen, Y., Ahlatci, H. (2018). Effects of carbonaceous reinforcements on microstructure and corrosion properties of magnesium matrix composites. *Mater. Chem. Phys.*, 218: 182-188. <https://doi.org/10.1016/j.matchemphys.2018.07.050>

[9] Radha, R., Sreekanth, D. (2017). Insight of magnesium alloys and composites for orthopedic implant applications – a review. *J. Magnes. Alloy.*, 5(3): 286-312. <https://doi.org/10.1016/j.jma.2017.08.003>

[10] Phedy, P., Djaja, Y.P., Boedijono, D.R., Wahyudi, M., Silitonga, J., Solichin, I. (2018). Hypersensitivity to orthopaedic implant manifested as erythroderma: Timing of implant removal. *Int. J. Surg. Case Rep.*, 49: 110-114. <https://doi.org/10.1016/j.ijscr.2018.06.011>

[11] Zhang, L., Xu, M., Hu, Y., Gao, F., Gong, T., Liu, T., Li, X., Pan, C. (2018). Biofunctionization of biodegradable magnesium alloy to improve the in vitro corrosion resistance and biocompatibility. *Appl. Surf. Sci.*, 451: 20-31. <https://doi.org/10.1016/j.apsusc.2018.04.235>

[12] Adetunla, A., Akinlabi, E. (2019). Improving the biocompatibility and corrosion resistance of AZ31 Mg alloy for biomedical applications. *MS&T19*, pp. 1-6. https://doi.org/10.7449/2019/MST_2019_291_297

[13] Rajkumar, K., Ramraji, K., Namratha, G., Manoj, S., Gnanavelbabu, A. (2020). A study of bio and tribo modifier on degradation of magnesium-calcium carbonate biomaterial. *Mater. Today Proc.*, 27: 691-695. <https://doi.org/10.1016/j.matpr.2019.10.165>

- [14] Vedabouriswaran, G., Aravindan, S. (2018). Development and characterization studies on magnesium alloy (RZ 5) surface metal matrix composites through friction stir processing. *J. Magnes. Alloy.*, 6(2): 145-163. <https://doi.org/10.1016/j.jma.2018.03.001>
- [15] Hashemi, R., Hussain, G. (2015). Wear performance of Al/TiN dispersion strengthened surface composite produced through friction stir process: A comparison of tool geometries and number of passes. *Wear*, 324-325: 45-54. <https://doi.org/10.1016/j.wear.2014.11.024>
- [16] Wu, H., Li, Y., Tang, X., Hussain, G., Zhao, H., Li, Q., Adedotun, A. (2015). Nano-mechanical characterization of plasma surface tungstenized layer by depth-sensing nano-indentation measurement. *Appl. Surf. Sci.*, 324: 160-167. <https://doi.org/10.1016/j.apsusc.2014.10.085>
- [17] A. K. Ghazi, N. K. Taieh, and S. K. Khudhur. (2022). Investigation of Dry Tribo-Behavior of Aluminum Alloy AA6061 / Al₂O₃ / Graphite Composites Synthesized by Stir Casting Technique. “*Revue des Composites et des Matériaux Avancés-Journal of Composite and Advanced Materials*”, 32(5): 253-259. <https://doi.org/10.18280/rcma.320506>